Journal of Physics: Conference Series **98** (2008) 062011 doi:10.1088/1742-6596/98/6/062011

Structural state and magnetic properties of $Nd_2Fe_{14}B$-type rapidly quenched alloys

N V Kudrevatykh[1], S V Andreev[1], A N Bogatkin[1], S G Bogdanov [2], A I Kozlov[1], P E Markin[1,2], O A Milyaev[1], A N Pirogov[2], V G Pushin[2] and A E Teplykh[2]

[1]Ural State University, 620083, Ekaterinburg, Lenin av., 51, Russia
[2]Institute of Metal Physics of RAS, 620219, Ekaterinburg, S.Kovalevskaya str., 18, Russia)

Nikolai.Kudrevatykh@usu.ru

Abstract. Using X-ray, elastic neutron diffraction (END) and small angular neutron scattering (SANS) methods (Diffractometers D2 and D3 respectively), transmitting electronic microscopy (JEOL JEM-200CX) and magnetometry technique (vibrating sample magnetometer -VSM) the structure and magnetic properties of the rapidly quenched (RQ) alloys of the following compositions: A) $Nd_{14}Fe_{78}B_8$; B) $Y_{12}Fe_{82}B_6$; C) $Nd_{13.3}$ $Co_{6.6}$ $Fe_{72.6}Ge_{0.9}$ $B_{6.6}$; D)$Nd_9Fe_{85}B_6$; E) $Nd_9Fe_{79}B_{12}$; F) $Nd_9Fe_{74}Ti_4C$ B_{12} have been studied. At some quenching conditions or after consequent heat treatments of these alloys the nanoscale state of the main 2-14-1 phase and α-Fe grains can be formed. Their size depends on the sample-preparation conditions and lies in the interval of 10–200 nm. Their influence on magnetic properties of alloys under study is discussed.

1. Introduction

From the moment of their discovery, hard magnetic materials based on neodymium-iron-boron system alloys have always been and currently are in the center of attention of researchers and technologists due to their outstanding hard magnetic properties [1,2]. The advantages of these materials originate from a high magneto- crystalline anisotropy and a high value of saturation magnetization of the main magnet material phase- $Nd_2Fe_{14}B$ (2-14-1). Over the last decade, numerous attempts have been made to obtain anisotropic powders of such materials for bonded magnets or to improve their magnetic properties through creation of exchange-coupled systems of nanosize particles of soft (α-Fe, Fe_3B) and hard (2-14-1) phases. It was shown in [3] that initial alloys with micrograin texture of 2-14-1 phase particles may be obtained by the centrifugal method in the process of melt quenching. This method allows anisotropic powders of the Nd-Fe-B alloy to be obtained for use as fillers for magnets with binders. Unfortunately, the degree of micrograin texture in this formed powder particles was not very high, which stimulated search for new methods of its raising. One of a possible way to achieve it would be in passing an electric current in the melt jet upon the spinning procedure. Indirect way is, of course, the obtaining such materials in completely amorphous state and subsequent thermo-mechanical treatment them under appropriate conditions [4].

We attempted to obtain R-Fe-B alloys of the following compositions: A) $Nd_{14}Fe_{78}B_8$; B) $Y_{12}Fe_{82}B_6$; C) $Nd_{13.3}Co_{6.6}Fe_{72.6}Ge_{0.9}B_{6.6}$; D)$Nd_9Fe_{85}B_6$; E) $Nd_9Fe_{79}B_{12}$; F) $Nd_9Fe_{74}Ti_4CB_{12}$ with nanograin structure by changing the surface chilling wheel speed, passing the electric current and annealing some samples

for the short time at relatively low temperatures. The results of the structure and magnetic properties investigation of the above mentioned objects are presented in this paper.

2. Experimental

Initial alloys were melted in an induction furnace, in Al_2O_3 or fused quartz crucibles. The ingots were then remelted in quarts ampoules with an orifice and subjected to the spinning (rapid quenching -RQ) at various surface speeds of the chilling wheel, $V_s = (10 \div 40)$ m/s.

Structural analysis was carried out by the X-ray diffraction method with the use of Cu-K_α radiation and transmission electronic microscopy (TEM), using JEM-200CX and CM-30 microscopes. Neutron scattering experiments were performed on the powder diffractometer D3 and the small-angle scattering device D6 (reactor IVV-2M, Zarechny, Russia). Incident neutron wavelengths were 0.243 and 0.478 nm for D3 and D6, respectively. The X-ray and neutron diffraction patterns analysis was performed using the FULLPROF package[5]. The magnetic properties were mainly investigated with the use of a vibrating-sample magnetometer (VSM) in a maximum field of 2T. All the samples were pre-magnetized under a pulsed magnetic field of 15 T prior to VSM measurements.

3. Results and discussion

The main phase of the investigated alloys samples is tetragonal with $Nd_2Fe_{14}B$-type structure. Impurity phases are NdB_4 $NdFe_2$ for A,C alloys and α-Fe for B,D,E,F ones. Amount of them does not exceed 5-20%.

Spinning of the all alloys gives rise to an amorphization. A content of crystalline phase always decreases with increase of the tangential wheel speed (quenching rate). The typical X-ray and neutron diffraction patterns of the A and C alloy samples (over and stoichiometric) in the initial and quenched states at V_s=40 m/s are shown in figure 1.

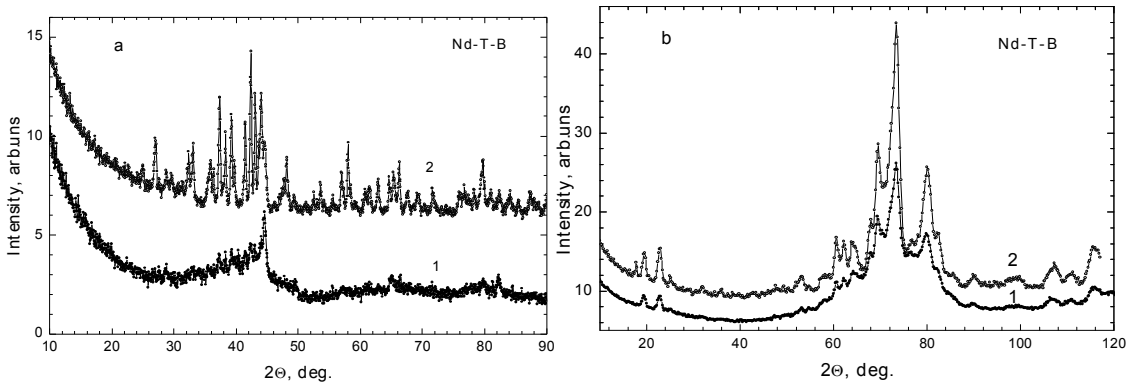

Figure 1. X-Ray (a) and neutron (b) diffraction patterns of Nd-Fe-Co-Ge-B (1 wt.% of Ge) sample quenched at V_S=40 m/s (1) and in crystalline state (2).

One can see that the structural peaks intensity in the quenched sample is significantly lower, and diffuse halos appear near the highest reflections. In figure 1b, the data are rescaled to the same exposition times and sample masses. Using the peak intensity data we estimated the amorphous phase volume in the sample to be equal to 60 %. The amount of crystalline phase was minimal in the sample quenched at a maximum rate. The existence of a mixture of soft and hard magnetic weakly exchange-coupled phases in the sample can also be inferred from the shape of the hysteresis loop shown in figure 2.

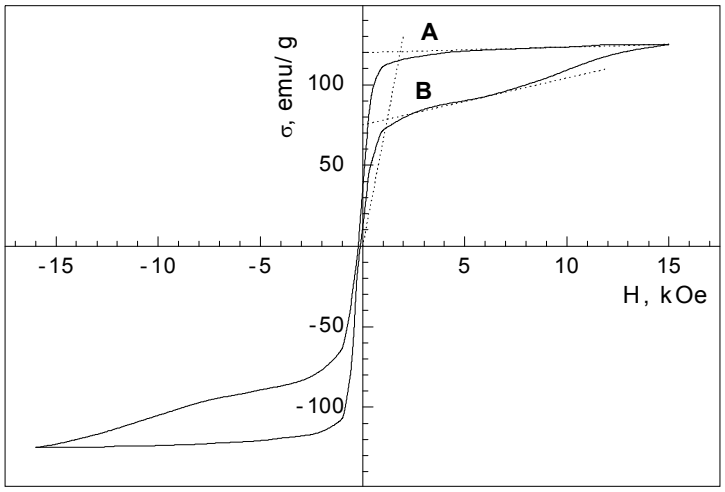

Figure 2. Hysteresis loop of Nd-Fe-Co-Ge-B alloy sample quenched at V_S=40 m/s.

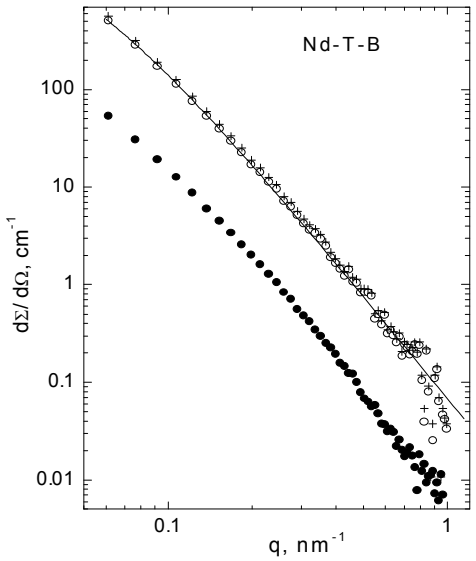

Figure 3. Angle dependences of SANS (cross crosses) and at 4 kOe (solid points) magnetic fields. The difference of cross sections in and without the magnetic field is shown with open circles.

We suppose these phases to be respectively amorphous and crystalline. As it follows from the positions of specific points A and B on the loop, the phase volumes ratio is 0.7: 0.3, which is in good agreement with the neutron diffraction data. The amorphous phase particle sizes were determined by the small-angle neutron scattering method (SANS) and compared with TEM ones. The SANS experimental data of the C-alloy sample (V_s=40 m/s) are presented in figure 3. Measurements were

fulfilled without and with an application of 4 kOe magnetic field. The field was applied parallel to the neutron scattering vector. We supposed that such the value of the magnetic field was sufficient for magnetizing of the amorphous phase.

Hence, a scattering in this case was caused by magnetic inhomogeneities of the crystalline phase, and probably, by atomic inhomogeneities of both phases.

This difference is shown in figure 3 with open circles. For its processing, we applied a model of a solid phase random distribution in sample[6]. Particle volume concentration c was taken from our neutron diffraction experiment, while particle size l and contrast ρ were determined from fitting of a model curve to the experimental cross sections. The calculated cross sections are shown in Fig. 3 with a solid line. We assume that the contrast arises due to difference of magnetizations in the crystalline and amorphous phases. We can thus estimate magnetization of soft magnetic phase σ_{am}. The values calculated from the experiment are given in table 1. TEM images of the RQ C-alloy structure are shown in Fig. 4. It is seen that the nanograins size determined from these analyses agrees well with the SANS data. (presented in table 1).

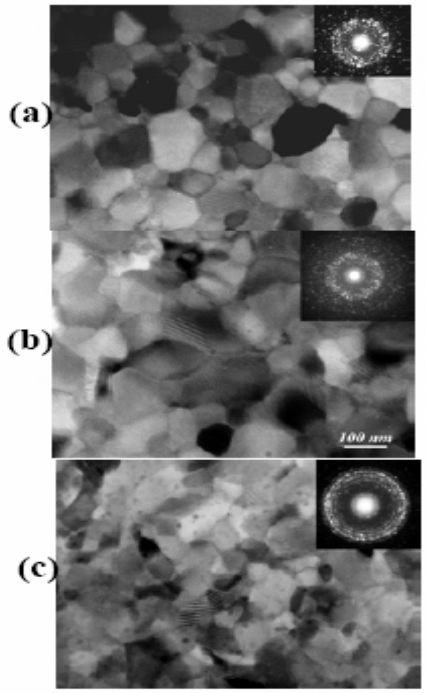

Figure 4. TEM bright field images of C-alloy samples taken from different ribbon parts and corresponding selected area diffraction patterns sections for C-alloy (V_s=40 m/s) at zero.

As it follows from the X-ray diffraction data, the main phase crystallizes in the tetragonal $Nd_2Fe_{14}B$-type structure. An impurity is α-Fe in the amount of 5-6 %. The lattice parameters and unit cell volume of the main phase grow with the quenching rate increase.

Samples of RQ $Y_2Fe_{14}B$ alloy The difference between the scattering curves, obtained in and without the magnetic field, describes were obtained at speeds V_s = 20, 30 and 40 m/s of the quenching wheel. In contrast of Nd-based alloys the spinning of $Y_2Fe_{14}B$ does not induce the amorphous phase. We observed a strong decreasing of reflection intensities with an increasing of speed of the cooling wheel, while reflections widths kept. We denoted a state of quenched $Y_2Fe_{14}B$ samples as defective one. In order to obtain information about defective phase content we measured the neutron reflection (101) of the crystalline sample (bulk alloy) and the quenched ones at various V_s (see Fig. 5).

Intensities were reduced to the same sample mass, exposition time and corrected for the absorption coefficient. This allowed us to estimate the quantity of the defective phase, which was equal to 10±5, 37±10 and 75±10 % for samples with V_s=20, 30 and 40 m/s, respectively. Particle sizes and contrast

were determined with the use of the same method as in case of the Nd system samples. The results are presented in table 1.

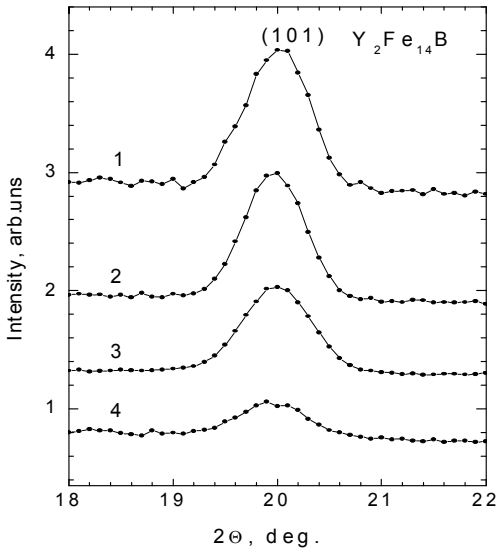

Figure 5. Neutron reflection (101) for $Y_2Fe_{14}B$ samples: crystalline (1) and quenched at V_s=20 (2), 30 (3) and 40 (4) m/s.

Table 1. Substructural and magnetic parameters of Nd-T-B (C) and $Y_2Fe_{14}B$ (B) samples.

Sample	V_p, m/s	*c*	*l*, nm	ρ, 10^{10} cm^{-2}	σ_{am}/σ_{cr}
Nd-T-B	40	0.6	50	0.85	0.71
$Y_2Fe_{14}B$	20	0.1	100	1.4	0.55
	30	0.37	40	0.33	0.89
	40	0.75	40	0.7	0.78
	crystal	0.02	240	3.1	

Magnetic hysteresis loops σ(H) measurements of quenched samples were carried out at 4.2 and 293 K. These measurements showed that the largest coercive force (H_c) values were observed in the 30 m/s sample: 1.0 kOe and 1.5 kOe at 4.2 and 293 K, respectively. Such the behavior of H_c(T) reasonably correlates with the magnetic anisotropy increase in the $Y_2Fe_{14}B$ compound in this temperature range [7]. It is worth notice that the effect of remanence enhancement in the isotropic uniaxial magnetic material above the level of 0.5 (σ_r/σ_s=0.55 at 4.2 K) was for the first time observed in this alloy. This ratio decreases to 0.45 at room temperature in spite of the coercivity increase.

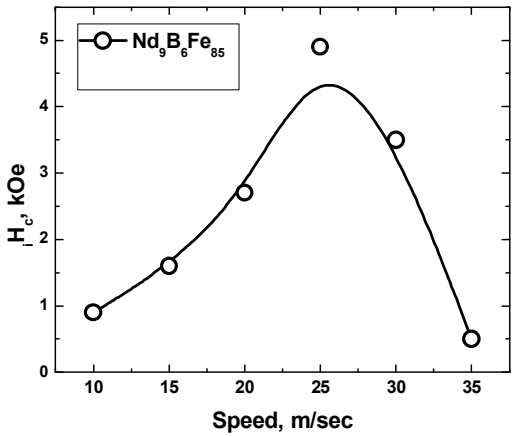

Figure 6. Coersivity dependence of RQ D-alloy samples on the chilling wheel surface speed.

The $H_c(V_s)$ dependence for the RQ D-alloy specimens shown in figure 6. It has a "bell like" view with the maximum value 5.0 kOe at V_s=25 m/s. TEM pictures and X-rays scans for the samples obtained at this and V_s= 35 m/s are shown in figures 7 and 9 respectively. One can conclude that the first sample possesses nanocrystalline structure containing the grains of 2-14-1 phase with the average size about 30 nm and more larger α-Fe grains dispersed in the interval 30 ÷200 nm. The D-alloy sample prepared at Vs=35 m/s has practically amorphous state (according TEM data). Its annealing during 5 min. in the temperature interval 510÷640 ^oC gives raise the H_c value up to 5.5 kOe. (figure 8). Corresponding microstructure of such sample shown in figure 7(3).

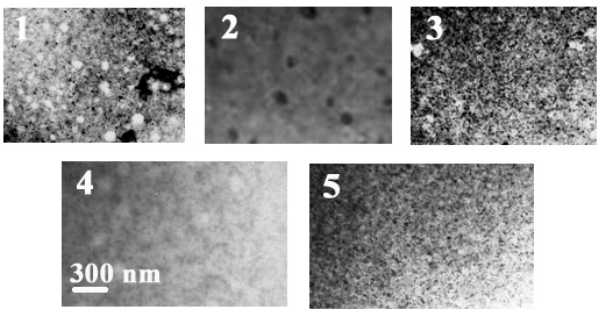

Figure 7. TEM bright field images of the RQ D-alloy samples prepared at: 1) V_s=25 m/s; 2) V_s=35 m/s; 3) V_s=35 m/s + T_{an}=640^oC; 4) V_s=35 m/s, I=-10 A; 5) V_s=35 m/s, I= +10 A..

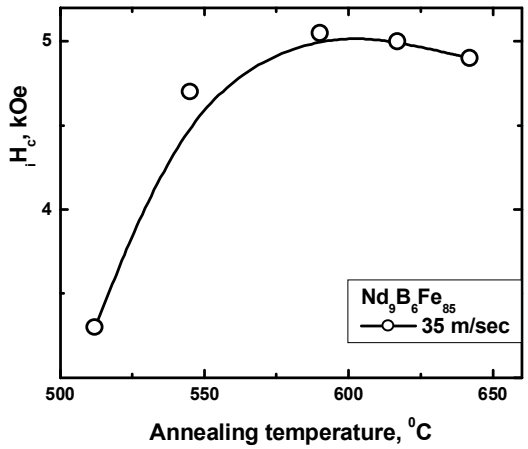

Figure 8. Coersivity dependence of RQ D-alloy samples prepared at V_s=35 m/s on the annealing temperature.

It is very interesting to note that the electrical DC current passing through the melt jet can drastically change the RQ sample structure and $_iH_c$ at the same V_s values with the positive electrical potential on the wheel but gives a very weak effect at the negative one (fig. 10, fig.7(4,5), fig. 9). The shape magnetic hysteresis loop difference for the RQ samples prepared at V_s=35 m/s with and without DC passing is seen evidently from fig. 11. The nature of this effect is not still clear.

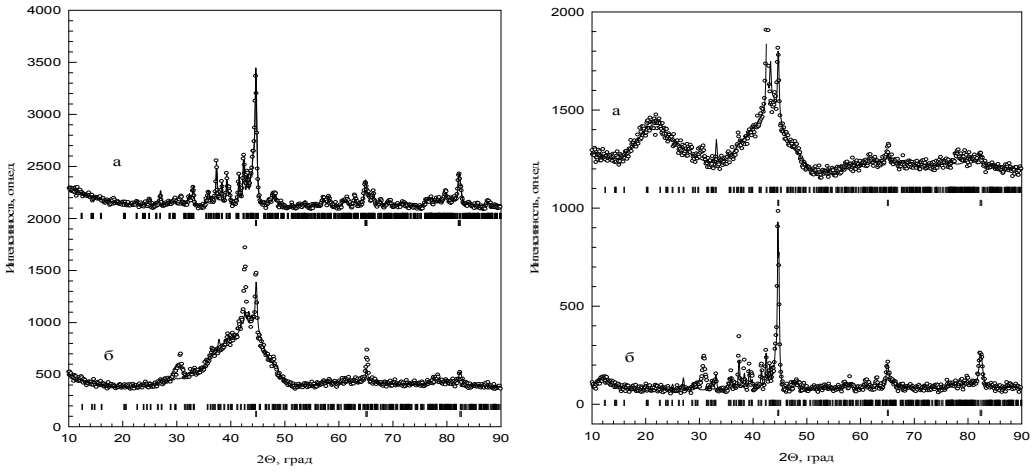

Figure 9. X-ray diffraction patterns from RQ D-alloy samples prepared at V_s=25 m/s (a); V_s=35 m/s (b); V_s=35 m/s I= -10 A (c); V_s=35 m/s I= +10 A (d)..

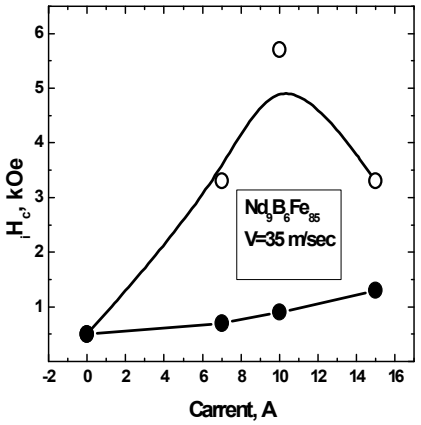

Figure 10. Coersivity values of D- alloy samples prepared at V_s = 35 m/sec as a function of electrical current polarity and intensity.

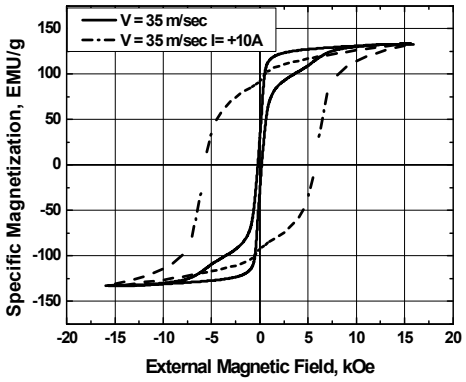

Figure 11. Magnetic hysteresis loops of RQ D-alloy samples prepared at V_s = 35 m/sec with.

Identical electrical DC current influence on the structure and magnetic properties of rapidly quenched A, C, E and F alloys was found also in this work. Details of this study will be published later.

The best magnetic properties parameters for the studied RQ alloys which we could attain in our investigation are listed in Table 2.

Table 2. The best attained magnetic parameters for the studied alloys at room temperature.

Alloy	σ_s EMU/g	σ_r UMU/g	$_iH_c$ kOe	$(BH)_{max}$ x 10^6GOe	Prepearing conditions
A		68	18	8,5	As spun
B	133	79	1.5	2.4	Annealing T=650°C, t=5min
C	121	92	17	14.0	Annealing T=550°C
D	132	116	6	16,5	Annealing T= 590°C t=5min
E	125	85	7,4	10,2	Annealing T=550°C t=5min
F	115	88	10,9	13,1	Annealing T=650°C t=5min

4. Conclusion

Through quenching by the centrifugal method, we however failed to obtain a Nd-T-B alloys of a composition close to 2-14-1 with nanograins texture or in fully amorphous state. The structural peaks of the quenched Y-based alloys are not broadened, for which reason we call the phase formed at quenching defective, rather than amorphous.

The SANS and TEM data show that the average size of the amorphous (or crystalline) inhomogeneities formed in the crystalline (or amorphous) matrix ranges between 10 and 200 nm. Such the structure is not optimal for obtaining a strong exchange coupling between 2-14-1 and α-Fe phase nanograins and high coercivity values attaining in the quenched alloys.

For the first time, we observed: 1) the effect of remanence enhancement in excess of 0.5 in the $Y_2Fe_{14}B$ alloy. prepared at the chilling wheel surface speed V_s=30 m/s; 2) the effect of drastically structure and magnetic properties change of the quenched alloys at the DC electric current passing through the melt jet upon the spinning procedure. The nature of this phenomenon is not still clear. Nevertheless this method using promises to improve hard magnetic properties of the quenched R-T-B type alloys applied as fillers for bonded magnets manufacturing.

Acknowledgements

This work was supported by the RF Science and Innovations Agency for Priority Direction Program "Industry of nanosystems and materials" (Project IN-12.3/001) and partly by High School Science Potential Development Program (project RNP 2.1.1.6945).

References

[1] Sagawa, S. Fujimura, M. Tagawa and Y.Matsuura, J. Appl. Phys. **55** (1984) 2083.
[2] R. Harris, P.Mc Guiness, C. Short, D. Book, O.Gutfleisch, A. Fujita, M. Verdier and H. Nagel, Trans. Mat. Res. Soc. Japan. **14**B (1994) 969.
[3] S.V. Andreev, N.V. Kudrevatykh et al.. J. Magn, Magn. Mater. **187** (1998) 83.
[4] G.P. Meisner, V. Panchanathan, J. Appl. Phys., **76** (10), (1994) 6259.
[5] J.Rodrigues-Garvajal, Physica B, 192 (1993) **55**.
[6] S. Bogdanov, E. Valiev, A. Pirogov et. al., Physica B, **350**, Suppl. 1, (2004), E1023-E1026.
[7] M.I. Bartashevich, N.V. Kudrevatykh et al., Sov. Phys. JETF, **97** (1990) 1985 (in Russian).